Statistics of Inelastic Torsional Responses of Single-story Asymmetric-plan Buildings

C.S. Lee & H. P. Hong
Department of Civil and Environmental Engineering, University of Western Ontario, Canada N6A 5B9

SUMMARY:
Torsional response caused by earthquake excitations can lead to non-uniform ductility demand on structural elements and severe damages. This response is significantly affected by the uncoupled torsional-to-lateral frequency ratio and the degree of torsional restraint of the system. This study is aimed at characterizing statistically the inelastic torsional behavior under bi-directional seismic excitations, and investigating the effects of uncoupled torsional-to-lateral frequency ratio, degree of torsional restraint and strength and stiffness degradations on the torsional responses. For the assessment, structures are modeled using simplified single-storey building under more than 350 ground motion records. The lateral load resisting elements for the single-story systems are modeled using the Bouc-Wen model. The torsional response is characterized using the torsional response ratio, defined as the response of a lateral load resisting element including the torsional effect to that by neglecting the torsional effect. The results show that the coefficient of variation of the ratio ranges from about 0.05 to 0.25, depending on uncoupled torsional-to-lateral frequency ratio. The trends of the mean of the ratio are given and discussed.
Keywords: Torsional response, bi-directional excitations, Bouc-Wen model

1. INTRODUCTION

The assessment of seismic torsional responses for structures could be important for seismic risk evaluation due to the non-uniform ductility demand on the structural frames induced by torsional effects. Literature reviews on the seismic torsional responses are given by Rutenberg (2002) and by De Stefano and Pintucchi (2008). The reviews indicated that although extensive research has been reported on tor-sional response, general and consistent conclusions are still of interest because a large number of parameters are needed to accurately characterize inelastic torsional responses. Perus and Fajfar (2005) attempted to explore the general trends in the seismic response of plan-asymmetric structures by using bilinear models and eight ground motion records. They indicated that the influence of using more realistic hysteretic models on torsional response should be investigated. De Stefano and Pintucchi (2010) investigated the features of inelastic torsional response by carrying out extensive parametric analysis and indicated that the investigation of effects of degradation of resisting elements on torsional response is needed. Furthermore, as the time-frequency energy distribution for different ground motion records could differ significantly. In most studies, the lateral load resisting elements are modeled using elasto-plastic or bilinear models and have been performed for a limited number of seismic records. Therefore, use of a large number of records and sophisticated hysteretic models to characterize the inelastic torsional responses and ductility characteristics under bidirectional excitations is needed.

This study is focused on the statistical characterizations of the inelastic torsional behavior under bidirectional seismic excitations. It investigates the influence of the lateral uncoupled frequency ratio, degree of torsional restraint and the degradations on the inelastic torsional responses for one-way asymmetric systems by considering the record-to-record variability. For the parametric studies, inelastic responses of simple single-story models are evaluated considering a set of 381 California records from 31 seismic events. The lateral load resisting elements are modeled using the phenomenological-based Bouc-Wen hysteretic model because it facilitates the consideration of the strength and stiffness degradations.

2. SINGLE-STORY MODEL AND ANALYSIS PROCEDURE

The idealized one-story model shown in Figure 1 has a rigid horizontal slab with uniformly distributed mass. The lateral load resisting elements are modeled using the Bouc-Wen hysteretic model (Wen 1976; Foliente 1995; Ma et al. 2004). They represent the frames or walls designed to resist the vertical force and the lateral load effects that are parallel to the elements. The center of mass (CM), center of stiffness (CS) located at (e_x, e_y), and the plastic centre (or center of strength) located at (e_{px}, e_{py}) are also shown in the figure.

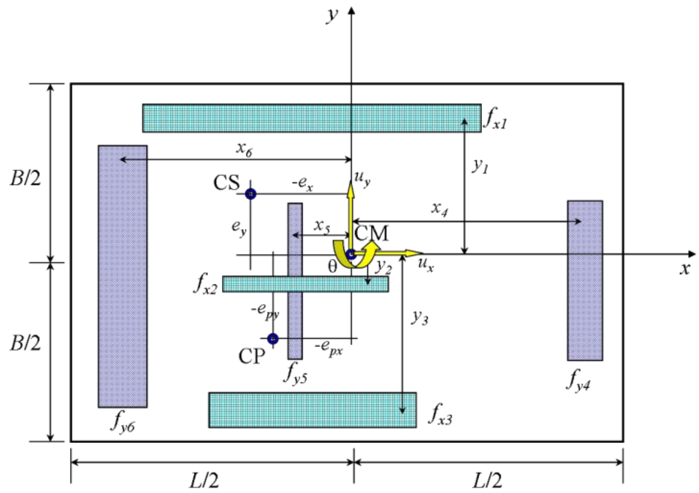

Figure 1. Idealized simple single-storey structure.

Let u_x, u_y and θ denote the displacement along *X*-axis, displacement along *Y*-axis and rotation of the rigid slab with respect to the CM. The equations of motion of the system with mass *m*, can be established (Chopra 2001; Ryan and Chopra 2004) as:

$$m\ddot{u}_x + c_x\dot{u}_x + \sum f_{xi} = -m\ddot{u}_{gx} \tag{1a}$$

$$m\ddot{u}_y + c_y\dot{u}_y + \sum f_{yi} = -m\ddot{u}_{gy} \tag{1b}$$

$$mr^2\ddot{\theta} + c_\theta\dot{\theta} + \sum(-f_{xi}y_i + f_{yi}x_i) = 0 \tag{1c}$$

where c denotes the damping coefficient, $\ddot{u}_g$ is the ground acceleration, f denote the resisting force of the element, an overdot on a variable denotes its temporal derivative, and the summation Σ is over applicable lateral load resisting elements. Symbols c and $\ddot{u}_g$ with an additional subscript *x*, *y* and θ are used to denote the quantities associated with the *X*-axis, *Y*-axis and rotation, respectively. f with subscript *xi* and *yi* denotes the resisting force along the *X*-axis and *Y*-axis, respectively, for the *i*-th lateral loading resisting element. Similarly, f with subscript *yi* denotes the resisting force along the *Y*-axis for the *i*-th lateral load resisting element. As the force-displacement relation for each lateral load resisting element is modeled using the Bouc-Wen hysteretic model, f_{xi} for the *i*-th lateral load resisting element (frame or wall) can be expressed as,

$$f_{xi} = \alpha_{xi}k_{xi}u_{xi} + (1-\alpha_{xi})k_{xi}z_{xi} \tag{2a}$$

where k_{xi} is the elastic lateral stiffness; α_{xi} is the ratio of the post-yield to initial stiffness; u_{xi} and z_{xi} are the displacement and hysteretic displacement, respectively; and z_{xi} is governed by (Wen 1976; Foliente 1995; Ma et al. 2004),

$$\dot{z}_{xi} = \frac{1}{\eta_{xi}}\left\{\dot{u}_{xi} - \nu_{xi}z_{xi}|\dot{u}_{xi}||z_{xi}|^{n_{xi}-1}[\beta_{xi} + \gamma_{xi}\,\mathrm{sgn}(\dot{u}_{xi}z_{xi})]\right\} \tag{2b}$$

where β_{xi}, γ_{xi}, and n_{xi} are the shape parameters; $\eta_{xi} = 1 + \delta_{\eta xi} E_{nxi}$; the parameter $\delta_{\eta xi}$ controls the stiffness degradation; $\nu_{xi} = 1 + \delta_{\nu xi} E_{nxi}$; the parameter $\delta_{\nu xi}$ controls the strength degradation; and the normalized dissipated hysteretic energy, E_{xi}, is defined by,

$$E_{xi} = \frac{(1-\alpha_{xi})}{Q_{xi}\Delta_{xi}} \int_0^t k_{xi} z_{xi} \dot{u}_{xi}\, dt = (1-\alpha_{xi}) \int_0^t \frac{z_{xi}}{\Delta_{xi}} \frac{\dot{u}_{xi}}{\Delta_{xi}}\, dt \tag{2c}$$

in which $\Delta_{xi} = (\beta_{xi} + \gamma_{xi})^{-1/n_{xi}}$ denotes initial yield displacement and $Q_{xi} = k_{xi}\Delta_{xi}$ is the initial yield force. Similarly, f_{yi} is defined by replace the subscript x with y in Eq. (2).

By assuming that the Rayleigh damping is applicable and the damping ratio for the two translational modes is identical and equal to ζ (= 5% is considered in this study) and considering that the model parameters α_{xi} and α_{yi} for the i-th lateral load resisting element are equal to α, Eq. (1) can re-written as,

$$\begin{Bmatrix} \ddot{\mu}_x \\ \ddot{\tilde{\mu}}_y \\ \ddot{\mu}_\theta \end{Bmatrix} + a_1\omega_x^2 \tilde{\mathbf{C}} \begin{Bmatrix} \dot{\mu}_x \\ \dot{\tilde{\mu}}_y \\ \dot{\mu}_\theta \end{Bmatrix} + \alpha\omega_x^2 \tilde{\mathbf{K}} \begin{Bmatrix} \mu_x \\ \tilde{\mu}_y \\ \mu_\theta \end{Bmatrix} + (1-\alpha)\omega_x^2 \begin{Bmatrix} \sum \kappa_{xi}\delta_{xi}\mu_{zxi} \\ \sum \Omega_y^2 \kappa_{yi}\delta_{yi}\mu_{zyi} \\ \frac{1}{r}\sum\left(-\kappa_{xi}\delta_{xi}\mu_{zxi} y_i + \Omega_y^2 \kappa_{yi}\delta_{yi}\mu_{zyi} x_i\right) \end{Bmatrix} = \frac{1}{\Delta_x} \begin{Bmatrix} -\ddot{u}_{gx} \\ -\ddot{u}_{gy} \\ 0 \end{Bmatrix} \tag{3}$$

where $\tilde{\mathbf{C}} = \begin{bmatrix} 1+\Omega_y & 0 & -e_y/r \\ 0 & \Omega_y + \Omega_y^2 & e_x\Omega_y^2/r \\ -e_y/r & e_x\Omega_y^2/r & \Omega_y + \Omega_\theta^2 \end{bmatrix}$,

$\tilde{\mathbf{K}} = \tilde{\mathbf{C}} + \Omega_y \mathbf{I}$, $\mathbf{I}$ denotes the identity matrix; Δ_x = min(Δ_{xi}) (Δ_{xi} is the yield displacement of the i-th element parallel to the X-axis); Δ_y = min(Δ_{yi}) (Δ_{yi} is the yield displacement of the i-th element parallel to the Y-axis); $\mu_x = u_x/\Delta_x$; $\tilde{\mu}_y = u_y/\Delta_x$; $\mu_\theta = r\theta/\Delta_x$; $\omega_x = \sqrt{K_x/m}$; $\omega_y = \sqrt{K_y/m}$; $\omega_\theta = \sqrt{K_\theta/mr^2}$; r is the radius of gyration of the slab with respect to the CM; $\Omega_\theta = \omega_\theta/\omega_x$ and $\Omega_y = \omega_y/\omega_x$ are used to denote the frequency ratios; $K_x = \sum k_{xi}$; $K_y = \sum k_{yi}$; $K_\theta = \sum\left(k_{xi}y_i^2 + k_{yi}x_i^2\right)$; $e_x = \left(\sum k_{yi}x_i\right)/K_y$ and $e_y = \left(\sum k_{xi}y_i\right)/K_x$ denote the load eccentricities measured along the X- and Y-axis; $\kappa_{xi} = k_{xi}/K_x$; $\kappa_{yi} = k_{yi}/K_y$; $a_1 = 2\zeta/(\omega_x + \omega_y)$; $\delta_{xi} = \Delta_{xi}/\Delta_x$, $\mu_{zxi} = z_{xi}/\Delta_{xi}$, $\delta_{yi} = \Delta_{yi}/\Delta_x$, and $\mu_{zyi} = z_{yi}/\Delta_{yi}$. The relations between μ_{zxi} and $\mu_{xi} = u_{xi}/\Delta_{xi}$ and between μ_{zyi} and $\mu_{yi} = u_{yi}/\Delta_{yi}$ for the i-th lateral load resisting element are governed by the Bouc-Wen hysteretic model, where $u_{xi} = u_x - \theta y_i$ and $u_{yi} = u_y + \theta x_i$.

We implemented the Bouc-Wen model in the FEAP (Taylor 2008), and Newmark's method is used to solve the governing equation (Eq. (1)). For the analysis, it is considered that the recording orientations of the first horizontal record component and the second horizontal record component coincide with the X- and Y-axes respectively.

The obtained normalized displacements μ_x and μ_y ($\mu_y = \tilde{\mu}_y \Delta_{x/y}$ and $\Delta_{x/y} = \Delta_x/\Delta_y$) represent the "global" ductility demands along the X- and Y-axis, respectively, if they are greater than unity; μ_{xi} (or μ_{yi}) represents the ductility demand for the i-th lateral load resisting element if it is greater than unity.

Before carrying out parametric study, we note that the dynamic characteristics of the structure are completely defined by ω_x, Ω_y, Ω_θ and the eccentricity ratios e_x/r and e_y/r, and the normalized responses are expressed as fractions of Δ_{xi}, Δ_{yi}, Δ_x and Δ_y. Furthermore, if the considered system is restrained in such a way that u_y and θ are zero, the system reduces to a single-degree-of-freedom (SDOF) system. For such a system and a given component of ground motion record, its normalized yield strength ϕ_x is, by definition, related to the yield displacement Δ_x by,

$$\Delta_x = \phi_x d_x \tag{4a}$$

where d_x is the peak linear elastic response of the corresponding linear elastic SDOF system for the considered record component, and can be evaluated without difficulty. d_x equals $S_x/(\omega_x)^2$, where S_x is the pseudospectral acceleration (PSA) for the first record component. Similarly, we have,

$$\Delta_y = \phi_y d_y \tag{4b}$$

and d_y equals $S_y/(\omega_y)^2$, where S_y is the PSA for the second record component.

Based on Eqs. (4a) and (4b), the vector on the left hand side of Eq. (3) can be re-written as,

$$\frac{1}{\Delta_x}\begin{bmatrix}-\ddot{u}_{gx} & -\ddot{u}_{gy} & 0\end{bmatrix}^T = \begin{bmatrix}-\ddot{u}_{gx}/(\phi_x d_x) & -\ddot{u}_{gy}/(\Delta_{x/y}\phi_y d_y) & 0\end{bmatrix}^T \tag{5}$$

For a given system and a ground motion record, the solution of Eq. (3) with the left hand side of Eq. (3) defined by Eq. (5) relates the normalized responses and the normalized yield strengths because d_x and d_y can be calculated from the corresponding linear elastic SDOF systems and for the given record, which simplifies the parametric study. The samples of the normalized responses for given values of ϕ_x and ϕ_y and a set of records can be obtained according to the following steps:

1) Compute d_x and d_y of the corresponding linear elastic SDOF systems for a given record;
2) Solve Eq. (3) to find μ_x, μ_y, θ, μ_{xi}, and μ_{yi};
3) Calculate the torsional response ratios R_{xi}, defined as μ_{xi}/μ_x, and R_{yi}, defined as μ_{yi}/μ_y to assess the torsional effects;
4) Repeat 1) to 3) for each considered record.

The samples can be used to assess the effect of the record-to-record variability on the statistics of the torsional response. Note that R_{xi} (or R_{yi}) <1.0 or >1.0 indicates that the rotational response leads to a decreased or increased translational displacement, respectively.

3. STATISTICS OF ELASTIC AND INELASTIC TORSIONAL EFFECTS

3.1. Considered ground motion records

For the assessment of inelastic responses of asymmetric structures, we use the same set of 381 California records from 31 seismic events that are considered discussed in Goda et al. (2009) and Lee and Hong (2010). The records are summarized in Table 1 according to the earthquake moment magnitude M, the distance D (km) (i.e., closest horizontal distance to the projected rupture surface on the earth), and the shear wave velocity in the uppermost 30 m, V_{s30} (m/s), representing soil conditions. The records are extracted from the Next Generation Attenuation Database (PEER Center, 2006), considering the high-pass filter corner frequency ≤ 0.2 Hz, and the low-pass filter corner frequency ≥ 10.

Table 1. Summary of California records used in the present study.

Grouped according to	Number of records (Total = 381)
M (Moment magnitude)	76 (M < 6.2), 189(6.2 ≤ M < 6.7), and 116 (M ≥ 6.7)
D (km)	109 (D < 15), 151 (15 ≤ D < 40), and 121 (D ≥ 40)
V_{s30} (m/s)	170 (V_{s30} ≥ 360) and 211 (V_{s30} < 360)

3.2. Statistics of the responses for a reference case

To assess the impact of the record-to-record variability on the torsional response, first, we consider a one-way asymmetric system with asymmetry about X-axis in stiffness with e_y/B = 0.1, $B = L$ and six lateral load resisting elements as illustrated in Figure 1. The uncoupled translational vibration period T_x (= $2\pi/\omega_x$) equals 0.5 (s). Three lateral load resisting elements that parallel the X-axis are placed at y equal to B/2, 0 and -B/2; the three elements that parallel the Y-axis are placed at x equal to B/2, 0 and -B/2. This considered case is referred to as the reference case. For the reference case, it is further considered that the uncoupled lateral and rotational natural frequencies are the same; the torsional restraints due to lateral load resisting elements parallel to the X-axis or the Y-axis are the same; the lateral load resisting elements have identical yield displacement (i.e., yield displacement constant type of elements or D-type elements (Tso and Myslimaj 2002)) and have the same Bouc-Wen model parameters; and ϕ_x and ϕ_y are equal. The torsional restraint of the structural system, γ_x and γ_y, defined by (Tso and Wang 1995, Paulay 1997),

$$\gamma_x = \frac{1}{K_\theta}\sum k_{yi}x_i^2, \text{ and } \gamma_y = \frac{1}{K_\theta}\sum k_{xi}y_i^2 \tag{6}$$

γ_x represents the contribution of the frames parallel to the Y-axis to the torsional capacity, and γ_y represents the contribution of the frames parallel to the X-axis to the torsional capacity. Table 2 summarizes these conditions, including the range of ϕ_x and ϕ_y. Note that the use of the D-type elements leads to the CP coinciding with the CS.

Table 2. Selected parameters for the reference case.

Dynamic characteristics	Ecc. & torsional parameters	Bouc-Wen model parameters	Normalized yield strengths
T_n=0.5(s) Ω_y=1, Ω_θ=1	e_x/L=0, e_y/B=0.1 e_{px}/L=0, e_{py}/B=0.1 γ_x=γ_y =0.5	α = 0, [$\beta_{\mu xi}$, $\gamma_{\mu xi}$, n_{xi}] = [0.5, 0.5, 2] for i = 4,5,6, [$\beta_{\mu yi}$, $\gamma_{\mu yi}$, n_{yi}] = [0.5, 0.5, 2] for i = 1,2,3	ϕ_x=ϕ_y $\in$ (0.1, 2)

Before presenting the statistics of the normalized responses for ranges of values ϕ_x and ϕ_y, we consider a particular set of values of ϕ_x and ϕ_y that are equal to 0.5 and 0.5. By carrying out the numerical analysis following the procedure described in the previous section for the mentioned 381 records, the correlation coefficient between one of the responses (μ_x, μ_y, μ_θ) and M, D, V_{s30}, S_x or S_y are calculated and shown in Table 3. The results shown in the table indicates that in all cases the correlation coefficient is less than 0.131, which is not very significant. Similar analyses and plots were carried out for other sets of ϕ_x and ϕ_y values, and the same observations to those drawn from Table 3 could be made. As the orientations of the considered records with small D values are not rotated to fault-normal orientation, the mentioned responses may not include the effect of near-fault motion. It is assumed that any possible dependence of μ_x, μ_y, μ_θ, R_{xi} and R_{yi} to M, D, V_{s30}, S_x and S_y as well as the near-fault can be ignored in the remaining part of this study.

Table 3. Correlation coefficients of samples for the reference case considering T_x = 0.5 and ϕ_x = 0.5.

Variable	R_{x1}	R_{x3}	μ_x	μ_y	μ_θ
M	-0.053	0.072	0.048	0.014	0.098
D (km)	-0.025	0.042	-0.04	-0.001	0.055
V_{s30} (m/s)	0.047	-0.063	0.004	-0.108	-0.03
S_x (g)	0.017	-0.08	-0.049	-0.054	-0.121
S_y (g)	-0.016	0.0085	0.023	-0.131	-0.04

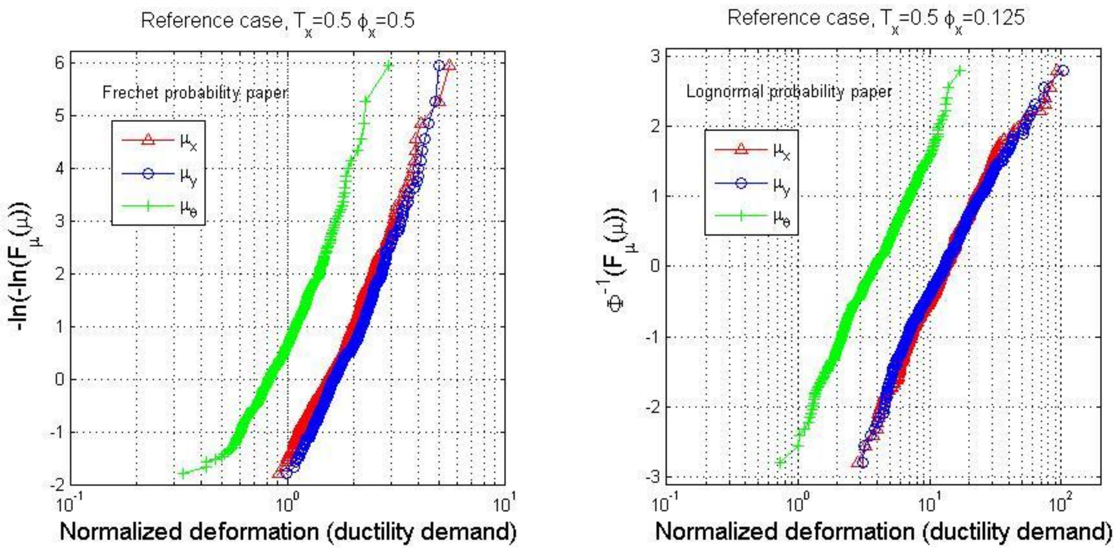

Figure 2. Empirical probability distributions of μ_x, μ_y and μ_θ presented on Frechet and Lognormal probability paper for the reference case.

To assign a probabilistic model to μ_x, μ_y, μ_θ and samples of these normalized responses are fitted to the lognormal model, and the Frechet model as one of these two models is preferred for a nonlinear SDOF system, depending on its vibration period (Hong and Hong 2007; Goda et al. 2009). Based on the statistical analysis and Akaike information criterion (AIC) or maximum likelihood criterion (Akaike 1974), it was concluded that, in general, the Frechet model and lognormal model is preferred depending on the values of ϕ_x. Illustrations of the samples for T_x = 0.5 and ϕ_x = 0.5 on Frechet probability paper, and T_x = 0.5 and ϕ_x = 0.125 on lognormal probability paper for are depicted in Figure 2.

3.3. Influence of torsional frequency ratio Ω_θ

First, we reconsider the reference case but replacing Ω_θ = 1.0 with Ω_θ = 0.8 (representing a torsionally flexible system) or with Ω_θ = 1.5 (representing a torsionally stiff system). Following the same procedure as for the reference case, the mean and the cov values of R_{xi} for Ω_θ = 0.8 to 1.5 are estimated and are shown in Figures 3 and 4, respectively. Major observations from the figures are:

1) When system responds linearly or with light to moderate nonlinearity ($\phi_x \geq 0.5$), the mean of R_{x1} decreases as Ω_θ increases and the mean of R_{x3} reaches the maximum for Ω_θ = 1 and decreases as Ω_θ increases if Ω_θ >1. However, when system responds with moderate to high nonlinearity (ϕ_x < 0.5), the influence of torsional frequency ratio is not significant.
2) The cov value of torsional response ratios increases as torsional frequency ratio Ω_θ decrease as well as normalized yield strength ϕ_x decrease. The magnitude of cov of R_{x1} and R_{x3} are ranged from 0.05 to 0.25.
3) As ϕ_x decreases, R_{x1} and R_{x3} tend to unity, implying that the torsional effect decreases. These observations indicate that the torsional effect is not significant as the system responds deep in the nonlinearly range. This is in agreement with those reported by Lucchini et al. (2009) for systems under unidirectional excitations.

3.4. Influence of torsional frequency ratio Ω_θ

To investigate the effect of degree of torsional restraint on the torsional responses, we take the same parameters as those for the reference case, except γ_x = 0.5 is replaced by γ_x = 0.33 or γ_x = 0.66. Similar to the previous sections, the mean and cov values of R_{xi} and R_{yi} are calculated and are shown in Figures 5 and 6. Inspection of the results shown in the figures indicates that the change in the torsional restraint does not affect the mean and cov values of R_{x1} and R_{x3} significantly. It must be emphasized that the results shown in the figures are for systems with the elements of D-type.

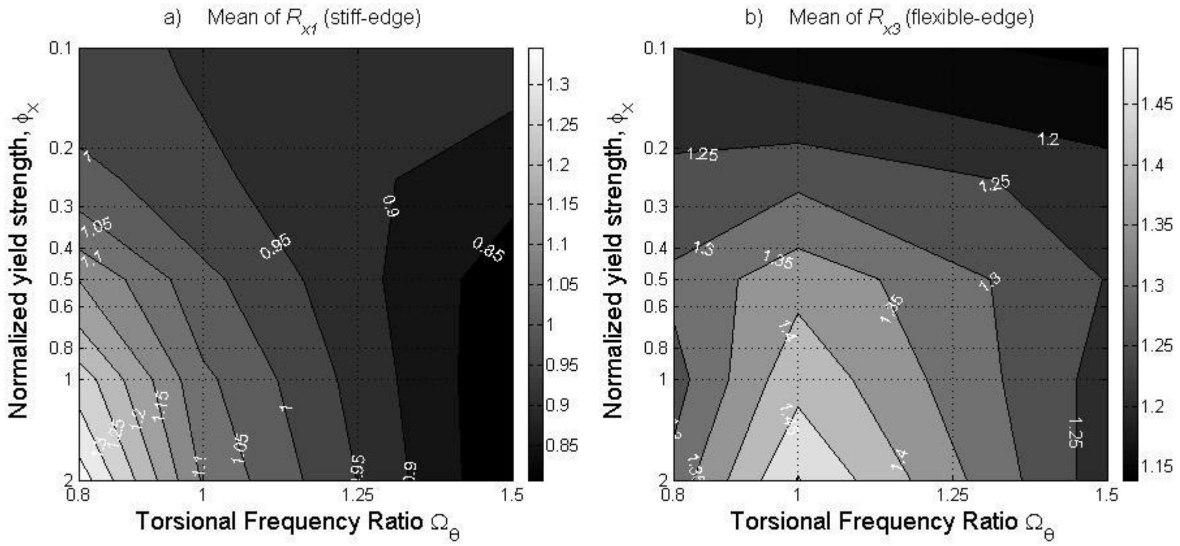

Figure 3. Mean of R_{x1} and R_{x3} for different values of torsional frequency ratio Ω_θ.

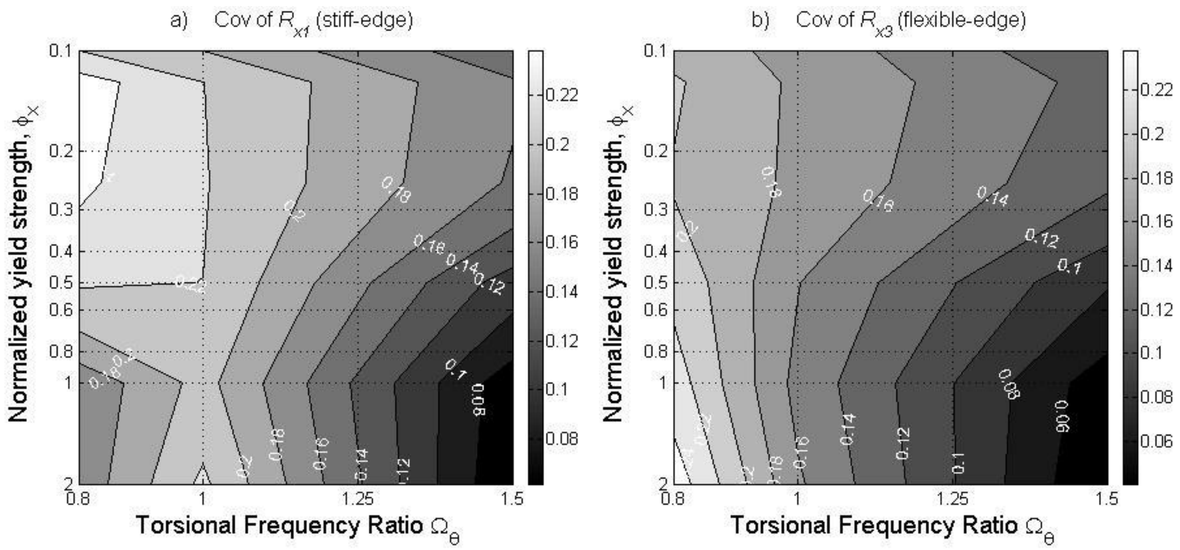

Figure 4. Coefficient of variation of R_{x1} and R_{x3} for different values of torsional frequency ratio Ω_θ.

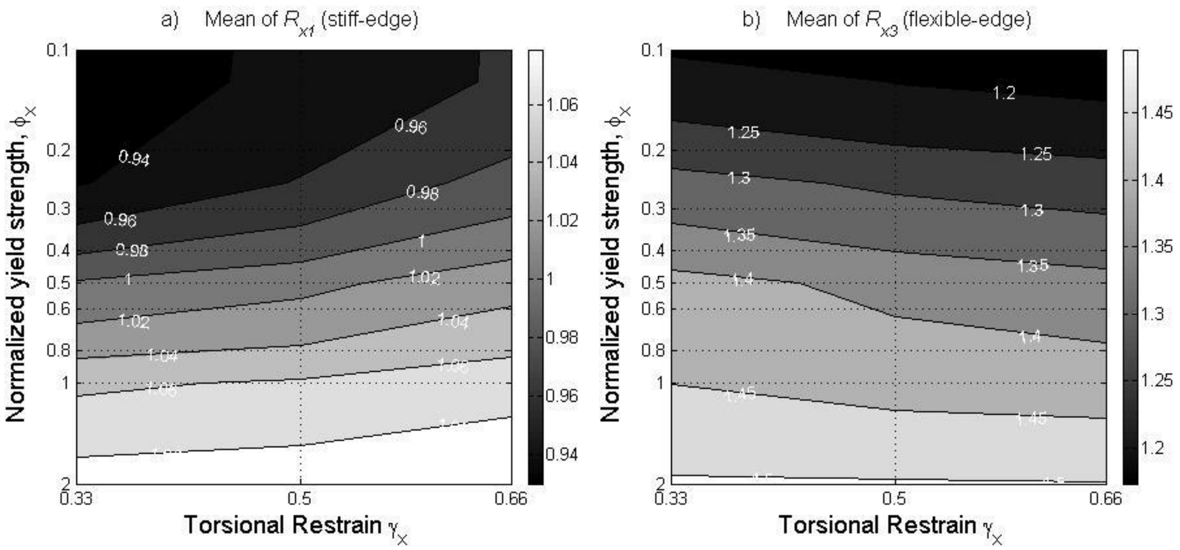

Figure 5. Mean of R_{x1} and R_{x3} for different values of torsional restraint γ_x.

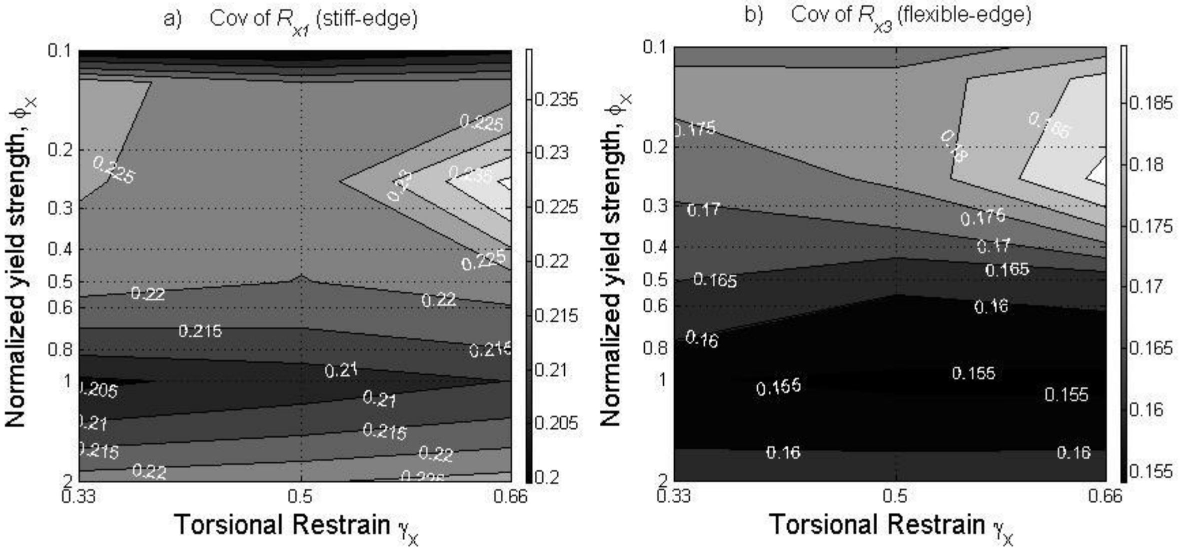

Figure 6. Coefficient of variation of R_{x1} and R_{x3} for different values of torsional restraint $\gamma_{x.}$

3.4. Influence of the strength and stiffness degradations

The influence of strength and stiffness degradations on the torsional behaviour is investigated by including the degradations in the reference case. However, to reduce the number of parameters, it is considered that the parameters of strength and stiffness degradations for each of the lateral load resisting elements ($\delta_{vxi} = \delta_{vyi} = \delta_{\eta xi} = \delta_{\eta yi}$) are identical and take a value ranging from 0 to 0.3. The estimated mean and cov of R_{xi} are shown in Figures 7 and 8. The results shown in Figures 7 and 8 indicate that the degradation affects negligibly the statistics of R_{x1} and R_{x3}.

Note that the observations made from Figures 7 and 8 may not be generalized as the degree of degradation for different systems could differ.

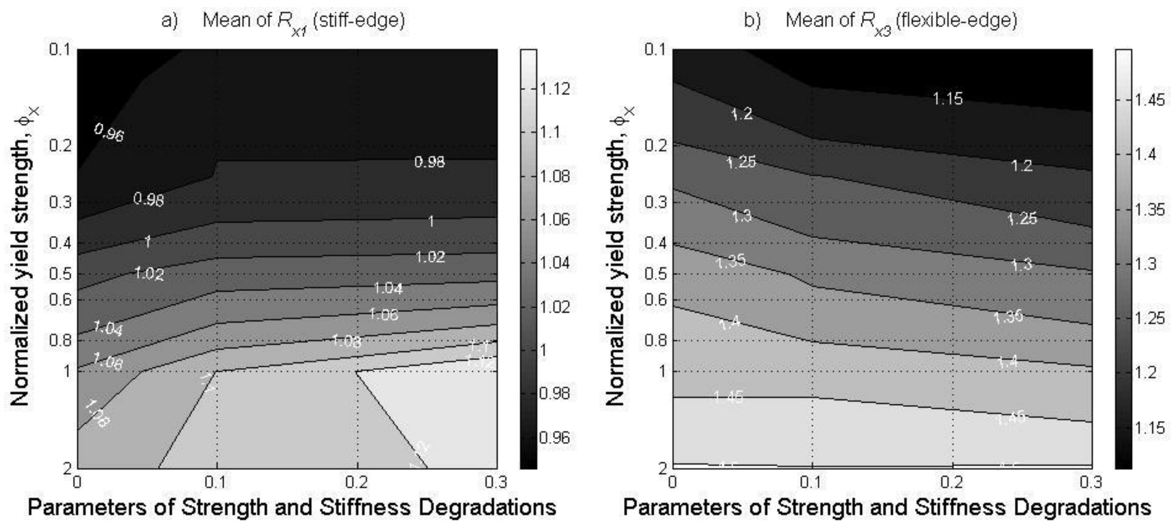

Figure 7. Mean of R_{x1} and R_{x3} for different values of parameters of strength and stiffness degradations

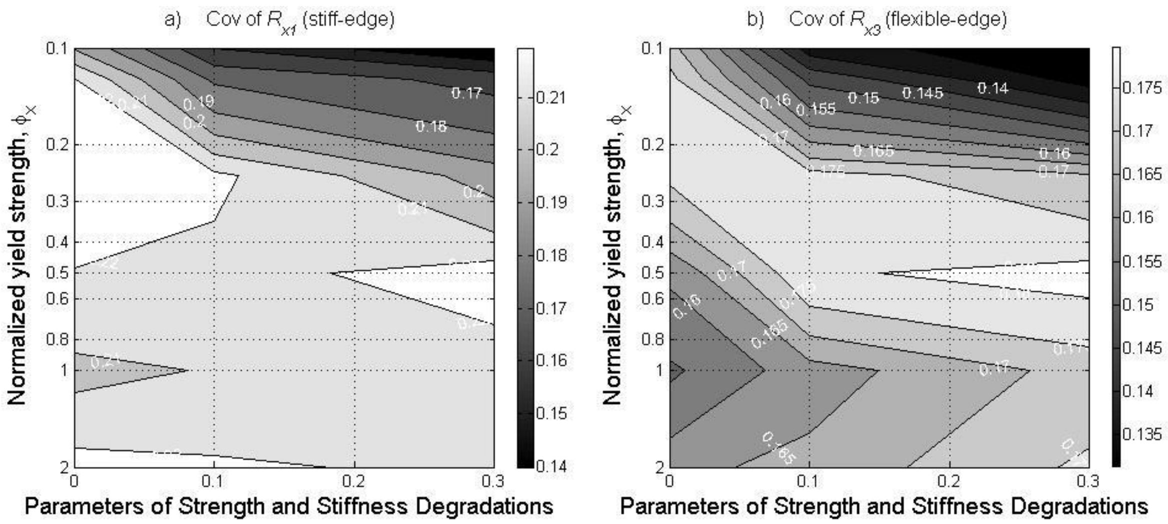

Figure 8. Coefficient of variation of R_{x1} and R_{x3} for different values of parameters of strength and stiffness degradations

4. CONCLUSIONS

To provide a statistical characterization of torsional response under bidirectional excitations caused by uncertainty in earthquake excitations, parametric studies are carried out for idealized single-story models using 381 records from California earthquakes of significant magnitude. For the analysis, the lateral load resisting elements are modeled using the Bouc-Wen hysteretic. In all cases, the torsional effect is characterized using the statistics of the ratio of the displacement of the lateral load resisting element to the displacement of the center of mass along the same direction. Based on the results of nonlinear dynamic analysis, it is concluded that:

a) If the system responds linearly or with light to moderate nonlinearity, the torsional effect in stiff-edge decreases as uncoupled torsional-to-lateral frequency ratio increases. The torsional effect in flexible-edge reaches the maximum if the uncoupled torsional-to-lateral frequency ratio equals unity. However, if the system responds with moderate to high nonlinearity, the influence of the uncoupled torsional-to-lateral frequency ratio on torsional effect is not significant;
b) The torsional response ratio tends to unity as the system responds deep in the nonlinear range;
c) The record-to-record variability leads to the values of the coefficient of variation (cov) of the torsional response ratios ranging from 0.05 to 0.25. The lower value is associated with linear responses of torsionally stiff system, while the upper value corresponds to the torsionally flexible systems.
d) For the systems under bi-directional excitations, the influence of the degree of torsional restraint on the torsional effect is not significant.
e) The consideration of strength and stiffness degradations does not affect the statistics of the torsional response ratios significantly.

AKCNOWLEDGEMENT

The financial support received from the Natural Science and Engineering Research Council of Canada and the University of Western Ontario is gratefully acknowledged.

REFERENCES

Akaike, H. 1974. A new look at the statistical model identification. *IEEE Transactions on Automatic Control*; 19: 716–723.

Chopra, A.K. 2001. *Dynamics of structures: theory and applications to earthquake engineering* (2nd ed.). Prentice Hall, N.J

De la Llera, J. C. and Chopra, A. K. 1995. Estimation of accidental torsion effects for seismic design of

buildings. *Journal of Structural Engineering*, *ASCE* 121(1):102–114.
De Stefano, M. and Pintucchi, B. 2008. A review of research on seismic behaviour of irregular building structures since 2002. *Bull. Earthquake Eng*. 6:285–308.
De Stefano, M. and Pintucchi, B. 2010. Predicting torsion-induced lateral displacements for pushover analysis: Influence of torsional system characteristics *Earthquake Engineering and Structural Dynamics*. DOI: 10.1002/eqe.1002.
Ellingwood, B. R., Galambos, T. V., MacGregor, J. G. and Cornell, C. A. *Development of a probability based load criterion for American national standard A58*. National Bureau of Standards Special Publication No. 577, Washington, D.C.; 1980.
Frankel, A., Mueller, C., Barnhard, T., Perkins, D., Leyendecker, E.V., Dickman, N., Hanson, S., and Hopper, M. *National seismic hazard maps*. Open-File 96-532, U.S. Department of the Interior, U.S. Geological Survey, Denver, CO.; 1996.
Foliente, G.C. 1995. Hysteresis modeling of wood joints and structural systems. *Journal of Structural Engineering* 121(6):1013–1022.
Goda, K., Hong, H.P. and Lee, C.S. 2009. Probabilistic characteristics of seismic ductility demand of SDOF systems with Bouc-Wen hysteretic behavior. *Journal of Earthquake Engineering* 13:600–622.
Hong, H. P., Goda, K. and Davenport, A. G. 2006. Seismic hazard analysis: a comparative study. *Canadian J. Civil Eng*; 33(9): 1156–1171.
Hong, H. P. and Hong, P. 2007 Assessment of ductility demand and reliability of bilinear single-degree-of-freedom systems under earthquake loading. *Canadian J. Civil Eng* 34(12): 1606–1615.
Humar, J. L. and Kumar, P. 1998. Torsional motion of buildings during earthquakes II Inelastic response. *Canadian Journal of Civil Engineering* 25(5)**:**917–934.
Lee, C.S., and Hong, H.P. 2010. Inelastic Responses of Hysteretic Systems under Biaxial Seismic Excitations. *Engineering Structures* 32(8):2074-2086.
Lucchini, A. Monti, G. and Kunnath, S. 2009. Seismic behavior of single-story asymmetric-plan buildings under uniaxial excitation. *Earthquake Engineering and Structural Dynamics* 38:1053–1070.
Ma, F., Zhang, H., Bockstedte, A., Foliente, G.C. and Paevere, P. 2004. Parameter analysis of the differential model of hysteresis. *Transactions of the ASME* 71(3), 342–349.
Pacific Earthquake Engineering Research (PEER) *Center Next Generation Attenuation database*. http://peer.berkeley.edu/nga/index.html. (last accessed April 4th, 2006).
Paulay, T. 1997. Are existing seismic torsion provisions achieving the design aims? *Earthquake spectra* 13(2):259–279.
Peruš I., Fajfar P. 2005. On the inelastic torsional response of single-storey structures under bi-axial excitation. *Earthquake Engineering and Structural Dynamics* 34(8):931–941.
Rutenberg A. 2002. AEE Task Group (TG) 8: behaviour and irregular and complex structures–progress since 1998. *Proceedings of the 12th European conference on earthquake engineering* CD ROM. London;.
Ryan, K.L. and Chopra, A.K. 2004. Estimation of seismic demands on isolators in asymmetric buildings using non-linear analysis. *Earthquake Engineering and Structural Dynamics* 33(3):395–418.
Taylor, R. 2008. FEAP - *A Finite Element Analysis Program User Manual*. University of California at Berkeley, Berkeley, California.
Tso, W.K. and Wong, C. M. 1995. Seismic displacements of torsionally unbalanced buildings. *Earthquake Engineering and Structural Dynamics* 24:1371–1387.
Tso WK, Myslimaj B. 2002. Effect of strength distribution on the inelastic torsional response of asymmetric structural systems. *Proceedings of the 12th European Conference on Earthquake Engineering* Paper No. 081, London, U.K.
Wen Y.K. 1976. Method for random vibration of hysteretic systems. *Journal of Engineering Mechanics* 102(2):249–263.